High Current Cold Electron Source Based on Carbon Nanotube Field Emitters and Electron Multiplier Microchannel Plate

Raghunandan Seelaboyina and Wonbong Choi[1]
Nanomaterials and Device Lab, Department of Mechanical and Materials Engineering,
Florida International University, Miami, FL 33174, USA

ABSTRACT

In this work, we report the synthesis and field emission properties of carbon nanotube multistage emitter arrays, which were grown on porous silicon by catalytic thermal chemical vapor deposition. The emitter structure consisted of arrays of multiwall nanotubes (MWNTs) on which single/thin-multiwall nanotubes were grown. The structure was confirmed by TEM and Raman analysis. Higher field emission current ~ 32 times and low threshold field ~1.5 times were obtained for these structures in comparison to only MWNT arrays. The enhanced field emission results for these multistage emitters are a consequence of higher field concentration, which was ~3 times more than only MWNTs. In this work we also report a novel method to amplify electron emission from field emitters by electron multiplication. A microchannel plate positioned between the emitter cathode and the anode was utilized to enhance the field emission current.

Keywords: Carbon nanotubes, Multistage, Field emission, Microchannelplate, Electron source.

1 INTRODUCTION

Field emission (FE) is one of the most promising applications of carbon nanotubes (CNTs). The high aspect ratio (~1000) and atomically sharp apex of CNTs enhances the local field and lowers the threshold field for electron emission (~0.5-1V/μm) [1-2]. In addition to the geometrical features they posses high electrical, thermal conductivity and high chemical, temperature stability. All these unique properties make CNT a robust and stable field emitter [3]. Field emission displays (FED) [4], electron guns for next generation scanning electron microscopes (SEM) and transmission electron microscopes (TEM) [5], miniature x-ray tubes [6] and source for high powered microwave (HPM) devices [7] are some of the various CNT FE applications that have been demonstrated. For these applications various CNT synthesis methods and structures have been investigated. One of the factors for efficient field emission is the distance between CNTs, which should be greater than their height to minimize electric-field screening effect [8]. This has lead to the growth of vertically and spaced CNTs by application of electric field [9], plasma enhanced chemical vapor deposition (PECVD) [10] and nano template assisted thermal CVD [11]. To further improve the emitter performance i.e. low threshold electric field and high emission current, recent works [12-17] have demonstrated a novel emitter design consisting of smaller emitters on a larger one. The enhanced field emission properties of such structures termed as multistage are attributed to the enhanced field enhancement factor (β). A ratio of local field (E_L) around the emitter tip to applied electric field (E_a) and the overall β for multistage emitters can be expressed as a product of their respective field enhancement factors [12-13, 17].

The emitters in the previous studies consisted of CNTs grown on carbon cloth [12], silicon posts [14], porous silicon pillars [15], ZnO nanorods [16] and tungsten oxide nanowires on tungsten tip [13]. To the best of our knowledge this is the first report on field emission on CNT-CNT multistage structures i.e. single wall nanotubes (SWNTs) or thin-multiwall nanotubes (thin-MWNTs) on MWNTs. Here we report the synthesis of vertically oriented CNT multistage emitter periodic arrays by catalytic thermal CVD method and its field emission properties. The emitter structure consisted of arrays of MWNTs on which SWNTs/thin-MWNTs were grown, and the distance between each multistage pillar was controlled to have higher field emission performance.

Here we also report on a method for achieving high emission current from CNTs and electron multiplier microchannel plate (MCP). Micro channel plates are used in several applications including X-ray, astronomy, e-beam fusion studies, nuclear science [18] and high efficiency field emission displays [19]. Our novel approach of combining CNT emitters and MCP will provide several benefits. First MCP amplifies the emission current and second it also protects the CNTs from irreversible damage during vacuum arcing [20]. Operation of MCP is based on avalanche multiplication of secondary electrons, which are generated when incident electrons strike the channel walls of a MCP. A voltage applied across the ends of the MCP creates a field which accelerates the secondary electrons along the channel leading to avalanche multiplication.

2 EXPERIMENTAL

The porous-Si substrates for CNT growth were prepared by anodization of 2 inch diameter and 300 μm thick p-type Si<100> with a resistivity of 0.008-0.02 ohm-cm. Anodization was performed in an electrolyte under galvanostatic i.e. current-controlled conditions in a simple

[1]Corresponding author Tel: (305)348-1973, Fax (305)348-1932
E-mail address choiw@fiu.edu

o-ring Teflon cell in the dark [21]. The electrolyte consisted of a 1:1 mixture (by volume) of 48 wt% HF and 100% ethanol. An aluminum foil pressed on the backside of the sample served as an ohmic contact and a platinum wire served as counter electrode. Anodization was carried out at a rate of 10 mA/cm^2 for ~5 minutes resulting in a nano porous-Si layer with a pore diameter of ~15-20 nm. On the resulting porous-Si substrates iron (Fe) catalyst thin film (~10 nm) was sputtered through a shadow mask followed by annealing for ~12 hours at 300^{0}C. Annealing under these conditions was observed to improve the contact of Fe catalyst with the nanopores. In addition annealing was also observed to relieve the stress in the porous film thus avoiding cracking during the nanotube growth [11]. For the nanotube synthesis the annealed substrates were placed in the cylindrical quartz tube of the CVD system, followed by heating to 700^{0}C in Ar (~1000 sccm). After the temperature was stabilized at 700^{0}C, Ar was replaced with C_2H_2 (~1000 sccm, 40 minutes) precursor gas, followed by cooling to room temperature for ~2 hours. For SWNT/thin-MWNT nanotube growth on top of MWNTs, 'Fe' catalyst was deposited for ~5 minutes through a shadow mask aligned with the previously grown MWNT arrays. Resulting substrates were then placed in a thermal CVD and nanotubes were grown by flowing a mixture of CH_4 (~1000 sccm) and C_2H_4 (~5 sccm) for ~5 minutes at 900^{0}C. Morphology of the synthesized nanotubes was determined by scanning electron microscopy (SEM) and transmission electron microscopy (TEM). Raman spectroscopy was used to determine the degree of graphitization. Field emission measurements for the multistage emitters were performed with and without MCP. In all the experiments indium tin oxide (ITO) coated quartz screen printed with conventional green phosphor paste was used as anode and the vacuum level was maintained at ~5E-7 Torr. The inter-electrode distance (*D*) i.e. cathode-anode in experiments without MCP and cathode-MCP in experiments with MCP was maintained at ~900 μm.

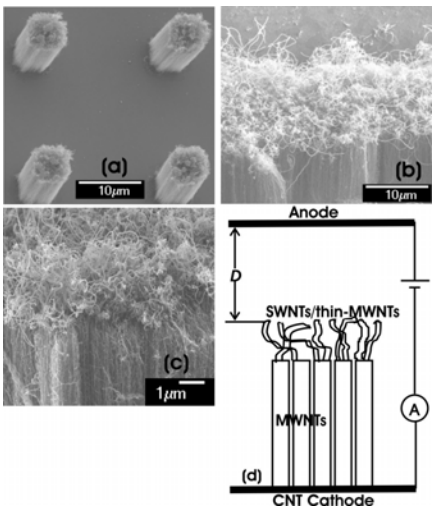

Figure 1. SEM images of (a) vertically oriented MWNT arrays grown on porous silicon; (b) MWNTs; (c) CNT multistage structure, i.e. thin MWNTs and SWNTs on top of MWNTs; (d) schematic of the multistage structure and field emission measurement schematic.

3 RESULTS AND DISCUSSION

Figure 1(a) shows the SEM image of vertically grown MWNTs on porous-Si nanotemplate. The growth mode of nanotubes on the porous-silicon is base growth mode similar to the one demonstrated by Fan et al [11]. This was verified by completely removing the nanotubes by reactive ion etching (RIE). Nanotube growth was observed on the resulting etched substrates without catalyst deposition, thus confirming the base growth (images not shown here). Vertical alignment for nanotubes grown on porous-Si nanotemplates is achieved by van der Walls force interaction between the adjacent nanotubes forming bundles with high rigidity from densely packed catalyst particles. The rigidity enables nanotubes to keep growing along the original direction i.e. normal to the substrate and even outermost nanotubes are held by inner nanotubes without branching away [11]. Length and diameter of the nanotubes were controlled by varying the precursor gas concentration and flow during the CVD growth. The average length and diameter of MWNT arrays grown for 45 minutes were ~55 μm and ~15-20 nm, respectively. The multistage structure of the CNTs seen in SEM image of figure 1c and schematic figure 1d can be distinguished by comparing with the top surface of MWNTs shown in figure 1b. The presence of smaller diameter nanotubes i.e. SWNT and thin-MWNT on top of the MWNT arrays i.e. multistage structure was determined from TEM and Raman spectroscopy. For TEM analysis few drops of suspension obtained from nanotube blocks sonicated in dichloroethane was deposited on a TEM grid. Figure 2a, 2b show the TEM images consisting of MWNT and thin-MWNT. The defective structure of thin-MWNT seen in figure 2b may be a result of lower growth time of ~5 minutes [16]. From the TEM analysis presence of SWNT was not found this may be due the modest amount of SWNT existence in the total sample, however their presence was confirmed from Raman spectroscopy. Usually radial breathing mode (RBM) peaks are not observed in MWNTs [22-23], however in our samples they were observed due to the presence of SWNT and thin-MWNT on top of MWNTs (figure 1c, d). The diameters (d_t) of nanotubes were calculated from the relation $d_t = 248/\omega_{RBM}$ [19], where ω_{RBM} is RBM frequency. The d_t values ranging from ~2.76-3.52 nm calculated for ω_{RBM} 50-150 cm^{-1} correspond to thin-MWNTs [23], d_t values ranging from ~1.28-1.96 nm for ω_{RBM} 125-200 cm^{-1} correspond to SWNTs [22] (figure 2a-c). The calculated d_t of nanotubes ω_{RBM} 50-200 cm^{-1} agreed well with internal diameters obtained from TEM analysis. The *G* band at ~1570 cm^{-1} of Raman spectra (figure 2c) indicates formation of graphene sheets and *D*-band peak at ~1344 cm^{-1} indicates defects or impurities [22] in the sample. The

NSTI-Nanotech 2008, www.nsti.org, ISBN 978-1-4200-8503-7 Vol. 1

average length and diameter of the SWNT and thin-MWNTs were ~10-15 μm and ~2-10 nm, respectively.

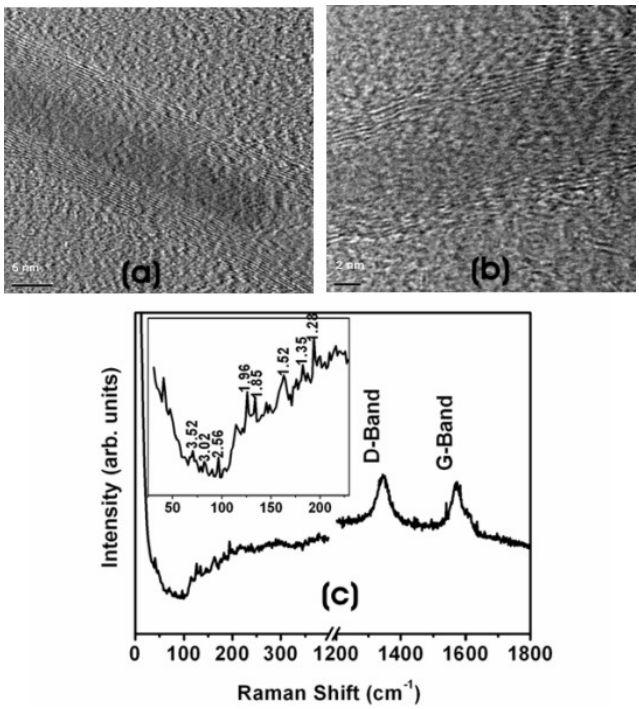

Figure 2. HRTEM images of (a) MWNTs and (b) thin MWNTs; (c) Raman spectrum (λ: 514 nm) of multistage CNTs with argon ion (Ar+) laser; inset, radial breathing mode (RBM) peaks, where inset numbers correspond to inner tube diameters of thin MWNTs and SWNT. Usually radial breathing mode (RBM) peaks are not observed in MWNTs [15]: however, in our samples they were observed due to the presence of SWNTs and thin MWNTs on top of MWNTs.

FE measurements of as-grown MWNT and multistage arrays at ~1 × 10^{-6} Torr are shown in figure 3. Obtained data was analyzed by Fowler-Nordheim (FN) equation [24], a relation between current (I) and applied electric field

$$I = \left(aA\beta^2 E^2 / \phi \right) exp\left(-b\phi^{3/2} / \beta E \right) \quad (1)$$

Where $a=1.54x10^{-6}\ A\ eV\ V^{-2}$ and $b=6.83x10^{7}\ eV^{3/2}\ V\ cm^{-1}$, respectively. A is emission area, β is field enhancement factor, E is applied electric field in $V\ cm^{-1}$ and ϕ is work function in eV. The turn-on field (E_t) and current at a field of 1 V/μm as seen in figure 3 for the multistage and MWNT arrays was ~0.4 V/μm, 0.6 V/μm and ~450 μA, 14 μA respectively. The lower turn-on field (~1.5 times) and higher emission current (~32 times) for multistage arrays can be attributed to its geometry, i.e. to higher field enhancement at the smallest nanotube tip on the vertically aligned MWNTs [12-13, 17]. The calculated β value from the slope of FN plot ($-b\phi^{3/2}D\beta^{-1}$) assuming ϕ 5 eV similar to graphite was ~ 26200 and ~8400 for multistage and as-grown MWNT arrays, respectively. The higher β (~3 times) value may also have resulted in higher field emission in multistage MWNT arrays [12-13]. Inset of figure 3 shows a fairly uniform emission image of the multistage arrays and the detailed investigation about their emission stability will be performed in future studies.

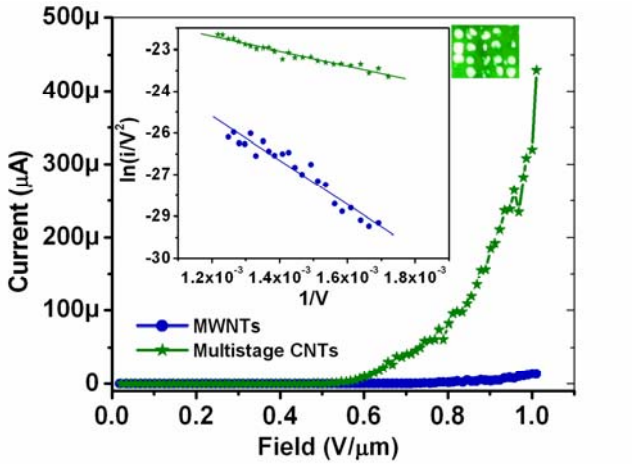

Figure 3. Emission current versus applied field plot, for multistage and MWNT arrays. Turn-on field (Et) was ~1.5 times lower and emission current was ~32 times higher for multistage in comparison to only MWNT arrays. Inset shows the corresponding FN plot and a fairly uniform emission image.

Electron multiplication was characterized by placing a commercial MCP (Hamamatsu) on top of the CNT cathode as represented by the drawing in figure 4b. The characterization was achieved by measuring the I-V data and by electron emission imaging. Schematic of the measurement circuit with and without MCP is shown in figure 4c. The 7.5 times higher (figure 4a) current with MCP is attributed to electron multiplication. So by placing an MCP on top of CNT emitters higher emission current could be achieved at moderate conditions. In both cases the turn-on voltages were approximately same. Enhanced emission current which was ~7.5 times higher with MCP can be attributed to electron multiplication. The commercial MCP plate placed on top CNTs amplified current by few micro amperes. However they are not suitable for achieving higher currents (few amperes) because of the lower secondary yield of the constituent materials. So a new MCP with stable and high secondary emission materials has been designed and fabricated which could be an efficient electron multiplier to achieve higher currents (data not shown here). This unique approach of placing the MCP over the field emitters could provide a more consistent and reliable cold electron sources operating at moderate power.

In summary, we have demonstrated synthesis and the field emission of vertically oriented multistage CNT arrays i.e. SWNTs/thin MWNTs on MWNTs on porous-Si and a reliable method for current amplification using a

microchannel plate. The enhanced field emission properties of CNTs in this study were a result of the multistage structure which produced ~3 times higher field concentration compared to only MWNTs. Current was amplified by 7.5 times with the microchannel plate positioned between the cathode and the anode.

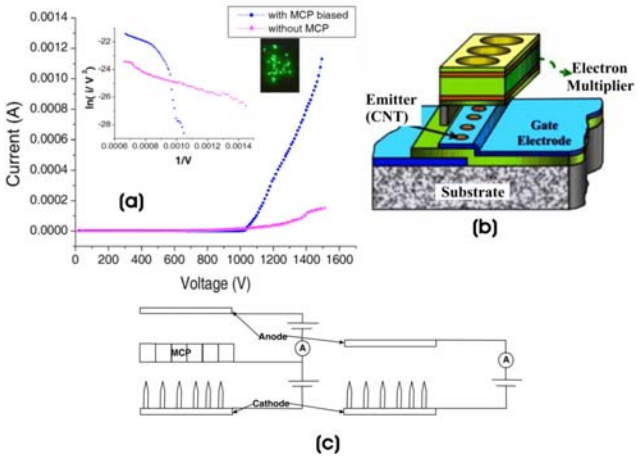

Figure 4(a) Emission current vs. applied voltage plot with and without MCP, (inset) FN plot and emission image with well defined spots (b) Schematic of a proposed novel cold cathode for high current density including carbon nanotube emitters and electrons multiplier microchannel plate, field emitted electron will be enhanced due to electro multiplication from MCP channels [patent pending] (c) schematic of measurement circuit with and without MCP.

REFERENCES

[1] Rinzler A G, Hafner J H, Nikolaev P, Lou L, Kim S G, Tomanek D, Nordlander P, Colbert D T, and Smalley R E , Science, 269,1550, 1995.

[2] Utsumi, T, IEEE Trans. Electron. Devices, 38, 2276, 1991.

[3] Seelaboyina R and Choi W B, Recent Patents on Nanotechnology, 1, 238, 2007.

[4] Choi W B et al, Appl. Phys. Lett., 75, 3129, 1999.

[5] De Heer W A, Chatelain A. and Ugarte D, Science, 270, 1179, 1995.

[6] Zhang J, Yang G, Lee Y Z, Chang S, Lu J P, and Zhou O, Appl. Phys. Lett., 89, 064106-1, 2006.

[7] Teo K B K, Minoux E, Hudanski L, Peauger F, Schnell J-P,Gangloff L, Legagneux P, Dieumegard D,Amaratunga G A J and Milne W I, Nature, 437 968, 2005.

[8] Nilsson L, Groening O, Emmenegger C, Kuettel O,Schaller E,Schlapbach L, Kind H, Bonard J-M and Kern K, Appl. Phys. Lett., 76, 2071, 2000.

[9] Chen L H, AuBuchon J F, Gapin A, Daraio C, Bandaru P, Jin S, Kim D W, Yoo I K and Wang C M, Appl. Phys. Lett., 85, 5373, 2004.

[10]Meyyappan M, Delzeit L, Cassell A, and David H, Plasma Sources Sci. Technol., 12, 205, 2003.

[11]Fan S S, Chapline M G, Franklin N R., Tombler T W, Cassell A M and Dai H, Science 283, 512, 1999.

[12]Huang J Y, Kempa K, Jo S H, Chen S and Ren Z F , Appl.Phys. Lett., 87, 053110, 2005.

[13]Seelaboyina R., Huang J, Park J, Kang D H, and Choi W B, Nanotechnology, 17, 4840, 2006.

[14]Hsu D S Y, and Shaw J, Appl.Phys.Lett., 80, 118, 2002.

[15]Li J X, and Jiang W F, Nanotechnology 18, 065203, 2007.

[16]Li C, Fang G, Yuan L, Liu N, Ai L, Xiang Q, Zhao D, Pan C, and Zhao X, Nanotechnology 18, 155702, 2007.

[17]Niemann D L, Ribaya D P, Gunther N, Rahman M, Leung J and Nguyen C V, Nanotechnology 18, 485702, 2007.

[18] Joseph Ladislas Wiza, Nuclear Instruments and Methods, 162, 587, 1979.

[19]Whikun Yi, Sunghwan Jin, Taewon Jeong, Jeonghee Lee, SeGi Yu, Yongsoo Choi, and J. M. Kim, Appl. Phys. Lett., 77, 1716, 2000.

[20]W. P. Dyke, J. K. Trolan, E. E. Martin, and J. P. Barbour, Phys. Rev., 91, 1043, 1953.

[21]Lehmanna V and Rönnebeck, S, Journal of The Electrochemical Society, 146, 2968, 1999.

[22]Dresselhausas M S, Dresselhaus G, Saito R, and Jorio A 2005 Physics Reports 409 47

[23]Seelaboyina R, Huang J and Choi W B 2006 Appl. Phys. Lett.88 194104

[24]Fowler R H and Nordheim L W 1928 Proc. R. Soc. A 119 173